Mechanochemical Activation of Copper Concentrate and the Effect on Oxidation of Metal Sulphides

SILVIANA ONISEI[1]*, VIOREL BADILITA[2], FLORIN STOICIU[2], TEODOR VELEA[2], VASILE PREDICA[2], CORNELIA LUPU[2], MIHAI BUTU[1], PETRU MOLDOVAN[1]

[1] University Politehnicaof Bucharest, Department of Engineering and Management for Elaboration of Metallic Materials, 313 Splaiul Independentei, 060042, Bucharest, Romania

[2] INCDMNR-IMNR, Bucharest, Romania, 102 Biruinţei Blv., 077145, Pantelimon, Romania

This work presents the effect of mechanochemical activation in an attrition mill, in water medium and for different time intervals, on the particle size distribution and microstructure of copper concentrate as well as, on the oxidation of the metal sulphides after treatment in an autoclave. Results show that the mean particle size decreased after 30 minutes of milling almost 10 times and the specific surface increased from 0.1 to 4.3 m^2/g. Regarding the micro-structural changes, it was found that during the mechanochemical activation the average crystallite size of chalcopyrite decreased, following an exponential trend towards a limiting value of approximately 20 nm, assuming spherical or equiaxed crystallites. The enhanced structural disorder of chalcopyrite is also highlighted by the linear increase of lattice strain with the milling time. Finally, results from the leaching experiments, demonstrated that the mechanical treatment improved the oxidation of sulphides by lowering the reaction temperature and increasing the reaction rates. The above data suggest that the mechanochemical activation of copper concentrate is an efficient method to enhance the hydrometallurgical oxidation of copper concentrate and chalcopyrite in particular.

Keywords: mechanochemistry, chalcopyrite, leaching, alkaline media

Currently, approximately 70% of world production of copper is obtained by pyrometallurgy which generates SO_2 and volatile dust and poses a high risk of environmental pollution [1]. On the other hand, extraction of copper from sulphide concentrates by hydrometallurgical processes has been a research topic that continues to attract scientific interest due to the environmental benefits.

As demonstrated, mechanochemical activation results in combined effects of increased surface area, vacancy and dislocations concentrations, grain boundaries, stacking faults and pores, structural disorder, metastable phases, higher oxidation states and alteration of the bond length/ angles/energy [2]. Milled materials transform into a metastable state, whose structure and reactivity essentially differ from the original one [3]. The use of X-ray diffraction line broadening measurements has been proved to be useful in the characterization of microstructure and structural characteristics [4, 5]. In terms of process changes, it results to lower reaction temperatures, increased reaction rate, increased dissolution and the formation of water soluble compounds. As a consequence, processing can be performed in simpler and less expensive reactors during shorter reaction times [6-8].

The effect of mechanochemical activation on the reactivity of sulphides has been studied by other researchers as well [9-11]. Achimovičová *et al.* have conducted experiments using chalcopyrite (deposit Slovinky, Slovakia) finding that mechanochemical treatment of the sulphides leads to increased reaction rate, improved leaching selectivity and sorption efficiency.

The purpose of this work is to study the effect of the mechanochemical activation on the micro-structure of copper concentrate and to determine how this is influencing the oxidation of the copper concentrate after autoclave treatment.

Experimental part

Materials and methods

Copper concentrate from Flotatia Baia de Aries (Romania) has been used for the experimental work and is denoted as CC1 00.

Chemical analysis was done with an atomic absorption spectrometer ZEEnit 700, Analytic Jena AG – Germany. Mineralogical analysis and microstructural changes have been made by X-ray diffraction (XRD) on a Bragg-Brentano Bruker D8 Advance diffractometer using the Bruker DIFFRAC^{plus} BASIC software, the ICDD database PDF-2 release 2006 and the WinFit software. X-ray diffraction data were carried out in the 2θ range from 4 to 74 degrees, 0.02 degrees step size and 0.3 s time per step with CuKα radiation at 40 kV and 40 mA. Optical microscopy was performed with Axiolmager A1m polarized light microscope. Particle size distribution was determined by Malvern MasterSizer Micro Plus laser diffraction.

Mechanochemical activation of copper concentrate was done using an Attritor MOLINEX mill. The volume of the vessel was 2 L, the stirrer rotation speed was 750 rpm whereas 2700 g of steel balls with diameter of 3 mm were used. Experiments were performed on samples of 200 g copper concentrate mixed with water at a ratio 2 to 1. The parameters for the mill were as follows: ambient temperature, ratio ball / lead concentrate: 13.5 to 1, milling time: 10, 20, 30 min. The un-milled sample was denoted as CC1 00. Mechanochemically activated samples are denoted as CC1 10, CC1 20 and CC1 30 for 10, 20 and 30 min of milling respectively. Leaching was done in a LA1000 autoclave with the following characteristics: vessel's maximum capacity 10 L, maximum temperature 250°C, maximum pressure 60 atm. The autoclave is equipped with an impeller stirrer driven by an engine with 1.1 kW power and 950 rpm maximum rotation speed. Experiments

* *Tel.: +400214029100*

Sample (wt.%)	Cu	Zn	Pb	Fe	Sb	As	Mg	Si	Ca	S	SO_4	LOI at 950°C
CC1 00	16.50	6.93	4.70	24.00	0.47	0.20	0.09	0.92	1.25	32.00	23.13	22.80

Table 1
CHEMICAL ANALYSIS OF THE COPPER CONCENTRATE CC1 00

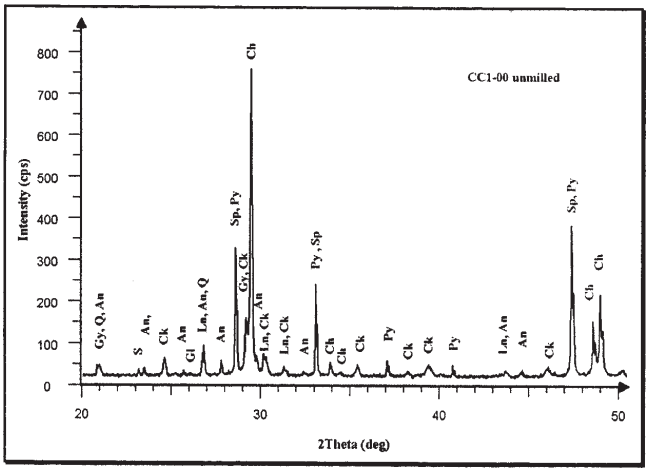

Fig. 1. Representative 2 theta region from the X-ray diffraction pattern of the sample CC1-00. Legend: Ch – Chalcopyrite; Py – Pyrite; Ck – Corkite; Sp – Sphalerite; Gy – Gypsum; An – Anglesite; S – Sulfur; Q – Quartz; Ln – Lanarkite; Gl - Galena

Compound Name	Formula	S-Q % (wt%)	PDF References
Chalcopyrite	$CuFeS_2$	47	00-037-0471 (*)
Pyrite	FeS_2	15	00-042-1340 (*)
Corkite	$PbFe_3(SO_4)(PO_4)(OH)_6$	12	01-080-0551 (N)
Sphalerite	ZnS	10	01-071-5975 (*)
Gypsum	$CaSO_4 \cdot 2H_2O$	6	00-033-0311 (*)
Anglesite	$Pb(SO_4)$	3	01-089-7356 (A)
Sulfur	S	3	01-078-1888 (*)
Quartz	SiO_2	2	01-070-7344 (*)
Lanarkite	Pb_2OSO_4	2	01-071-2069 (*)
Galena	PbS	<1	01-077-0244 (*)

Table 2
MINERALS IN THE COPPER CONCENTRATE CC1 00. S-Q %: SEMI-QUANTITATIVE.

Note that the major mineral is chalcopyrite and this cumulates practically all the copper from concentrate.

were performed on samples of 200 g copper concentrate and sodium carbonate solution at a ratio 1 to 15 and an excess of Na_2CO_3 30% more then stoichiometric necessary, in presence of air. Leaching experiments had been done on copper concentrate before and after milling for 30 min, at 100, 115 and 135°C.

Results and discussions

Characterisation of raw materials

The chemical composition of the copper concentrate used in the present study is shown in table 1.

The XRD phase analysis is presented in figure 1 and in table 2.

Microscopic analysis revealed the presence of the following minerals: chalcopyrite -$CuFeS_2$ (major phase), blenda - ZnS, galena - PbS, pyrite - FeS_2, tenantite – tetraedrit – $Cu_{12}(Sb,As)_4S_{13}$ (fig. 2). The minerals occur as individual grains or rarely, as polycrystalline aggregates (fig. 3). Tenantite-tetraedrit, a solid solution where Sb and As isomorphic substitute each other, sometimes appears as crystals with multiple areas (fig. 3), in which the central part presents the closest composition to tenantite (olive-grey) while the boundaries present tetraedrite form (green-grey). Galena is usually covered with a tire most probably composed by sulphates formed through alternating (figs.5 and 6).

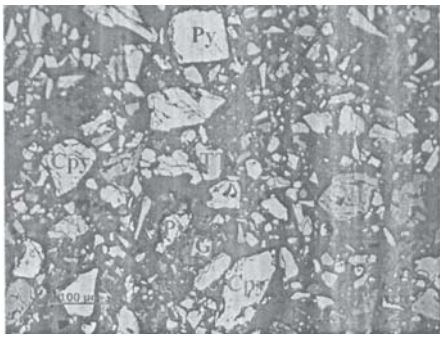

Fig. 2. Sample CC1 00, reflected light: Cpy-chalcopyrite, Py-pyrite, Bl-blenda, Gl-galena, a-sulfates tire, TT-tenantite-tetraedrit

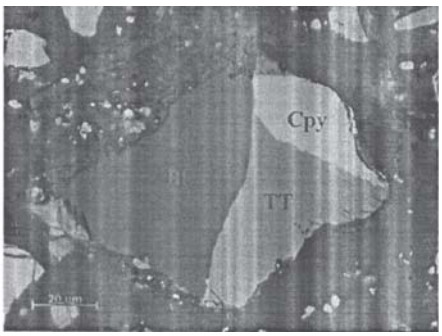

Fig. 3. Sample CC1 00, reflected light, immersion in cedar oil: Cpy-chalcopyrite, Bl-blenda, TT-tenantit-tetraedrit

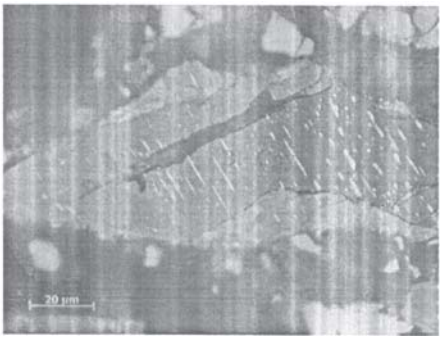

Fig. 4. Sample CC1 00, reflected light immersion in cedar oil: Bl-blende with chalcopyrite (Cpy)

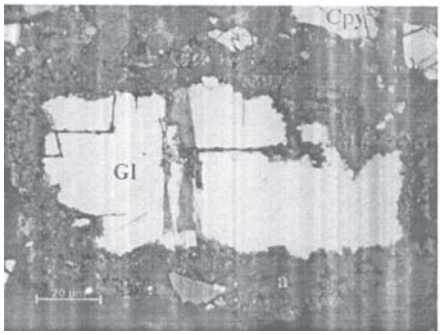

Fig. 5. Sample CC1 00, reflected light immersion in cedar oil: Cpy-chalcopyrite, Bl-blende, a-sulfates tire

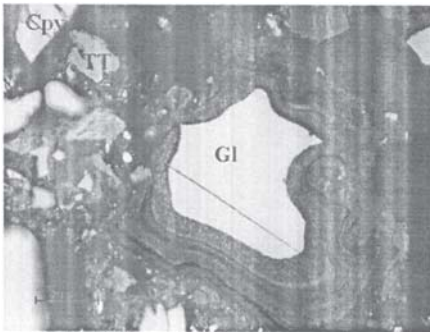

Fig. 6. Sample CC1 00, reflected light immersion in cedar oil: Bl-blende, Cpy-chalcopyrite, Gl-galena, a-sulfates tire, TT-tenantit-tetraedrit

In terms of particle size distribution, CC1 00 is characterized as a fine material, as 50 vol% of material is less than 100 μm and 80 vol% less than 320 μm (fig. 7).

Influence of mechanical activation time on particle size distribution and specific surface.

The evolution of particle size distribution after 10, 20 and 30 min of milling is depicted in figure 8.

The particle size distribution reveals that after 10 min of milling the mean size of the particles (d50) decreases from 99 to 20 μm and after 30 min milling time reaches 12.0 μm.

The specific surface for a granular material (powdered) can be determined by calculation (non-porous materials with an average grain size and coarse) and by BET method (Brunnauer Emmet Teller) for porous, fine materials. In this case the first method was chosen [12].

The specific surface is given by:

$$S = \frac{1}{100} \cdot \frac{Q}{\gamma} \cdot \sum \frac{\ln d_{i+1} - \ln d_i}{d_{i+1} - d_i} \cdot \Delta Z_i, \qquad (1)$$

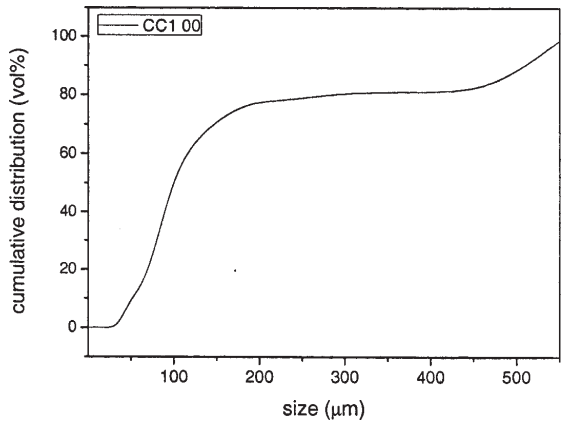

Fig. 7. Particle size distribution for CC1 00

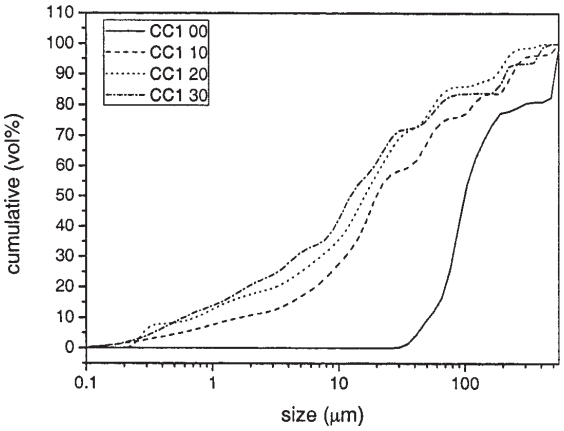

Fig. 8. Particle size distribution as a function of milling time

where:

d = diameter of particle;

Q = shape factor;

γ = specific weight [g/cm^3];

ΔZ_i = percentage composition for each class.

For results to be accurate a complete analysis of particle size distribution is required, especially for fine classes with a higher specific surface. Calculation of specific surface was made using the histogram from particle size distribution tables of the analysed samples. The results are depicted in table 3.

The specific milling energy was calculated using the Heegn relationship [KWh/t^{-1}] [13].

$$E_M = \left(\frac{m_1}{m_2}\right) \cdot n \cdot t \cdot g \cdot D \cdot \pi \cdot \mu(\nu) \qquad (2)$$

where:

m_1 = weight of balls [Kg];

m_2 = weight of sample [Kg];

n = grinding speed [s^{-1}];

t = milling time [s];

g = gravitational acceleration [9.81ms^{-2}];

D = diameter of milling chamber [m];

μ (ν) = coefficient of friction (0.90 for 2 mm diameter balls).

Results are presented in figure 9. As expected, the milling process becomes more energy demanding with the decrease in particle size. Indeed, the ratio specific milling energy to specific surface is increasing from 39 to 46 and 53 KWh*g/m^{2}t^{-1}, for 10, 20 and 30 min respectively.

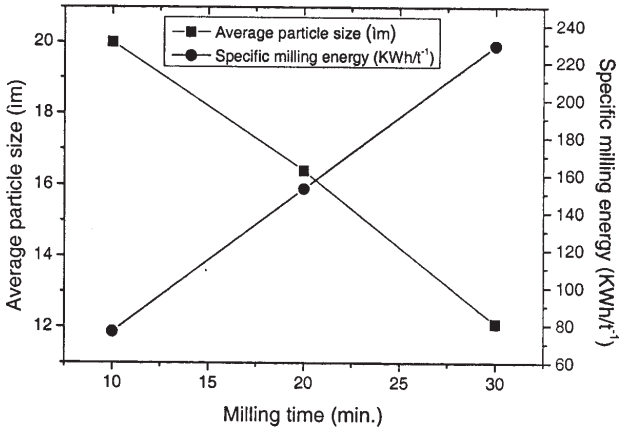

Fig. 9. Variation of specific milling energy as a function of specific surface and average particle size distribution

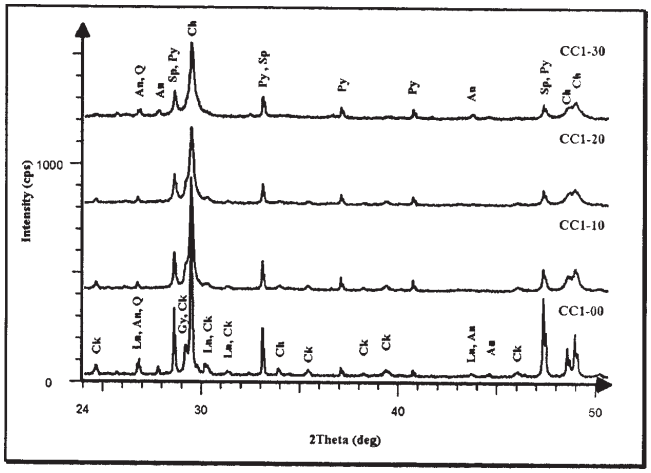

Fig. 10. X-ray diffraction for samples CC1-00, CC1-10, CC1-20, CC1-30

Influence of mechanical activation time on microcrystalline deformation

In figure 10, the X-ray diffraction scans for copper concentrate samples CC1 00, CC1 10, CC1 20 and CC1 30 are presented. This allows the assessment of the overall effects induced by mechanical activation of copper concentrate.

With increasing time of mechanical activation gradual broadening of all diffraction peaks is found. This indicates the decrease in crystallite size and the occurrence of microstrain for all the minerals present in the concentrate.

Depending on the concentration and on the properties of each mineral present in the starting material and also depending on the chosen parameters for mechanical activation, some minerals can't be detected by XRD at higher milling times. This is the case for the following minerals after 30 min of activation: Gypsum, Sulfur, Lanarkite, Corkite. This fact may be correlated with the amorphisation of these minerals due to ball milling, either by reducing the crystallite size (probably Sulfur, Lanarkite), either by solid state reactions (likely decomposition of Gypsum, Corkite).

Since most of the copper is linked to chalcopyrite, mechanical activation effects were highlighted by XRD only for this mineral. To validate the consistency of the results, two partially complementary methods were used in order to evaluate the effects of mechanical activation on the microstructure of Chalcopyrite: Full Pattern Matching (FPM) method from Bruker software EVA12 [14] and Voigt method line profile analysis with WinFit software [15].

It is known that the diffraction peak profile is determined by the instrumental parameters (characteristic of the device) and the physical parameters (characteristic of the sample studied). To separate the instrumental contribution and physical contribution, a standard reference material SRM 1976 [16] (a plate of corundum α-Al_2O_3) was used.

The selection of the reference material is based on its properties, as it is certified with respect to grain size, shape, microstrain, and texture. The profile of the diffraction peaks from SRM 1976 is determined only by the instrumental parameters.

FPM method allows the diffraction peak profiles to be described by an empirical model. In order to simulate peak profiles the asymmetrical pseudo-Voigt function was used. The use of this method allowed the determination of the lattice parameters of chalcopyrite and of the isotropic average crystallite size (in hypothesis of spherical or equiaxed crystallites), as a function of the duration of mechanical activation. The average size of a crystallite was calculated for a hypothetical peak located at 2θ = 30°, with the Scherrer formula, after eliminating the instrumental contribution to peak's shape and also ignoring peaks' profile broadening generated by the microstrains:

$$D = \frac{180}{\pi} \cdot \frac{k\lambda}{\sqrt{(B_t^2 - B_0^2)}} \cdot \frac{1}{\cos\theta} \quad (3)$$

where:

D means isotropic average crystallite size;

$180/\pi$ converts the FWHM (full width at half maximum) from degree to radians;

B_t is FWHM for studied material;

B_0 is the instrumental broadening, i.e. FWHM for a material (SRM 1976) that exhibits no broadening beyond the instrument contribution;

λ is the wavelength of the radiation; it is expressed in angström (A), D is thus also in A;

k is the Scherrer constant, (~ 0.9 meaning ratio between the FWHM and the IB (integral breadth) of the diffraction maximum);

θ is the diffraction angle.

The FPM method results are highlighted in table 4 and figure 10.

No.	Name	Milling time, (min)	Specific surface, (m^2/g)
1	CC1-00	0	0.11
2	CC1-10	10	1.95
3	CC1-20	20	3.34
4	CC1-30	30	4.33

Table 3
SPECIFIC SURFACE FOR 10, 20 AND 30 MIN OF MILLING

Time / min	0	10	20	30
Isotropic Crystallite Size (Scherrer) / nm	96.2	42.4	30.3	27.4
a / Å	5.2891	5.2881	5.2890	5.2880
c / Å	10.4213	10.4255	10.4253	10.4248

Table 4
SUMMARY OF FPM RESULTS

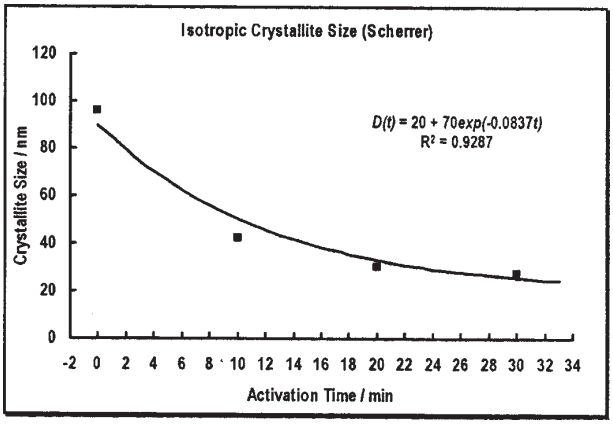

Fig. 11. Isotropic crystallite size of chalcopyrite vs. activation time

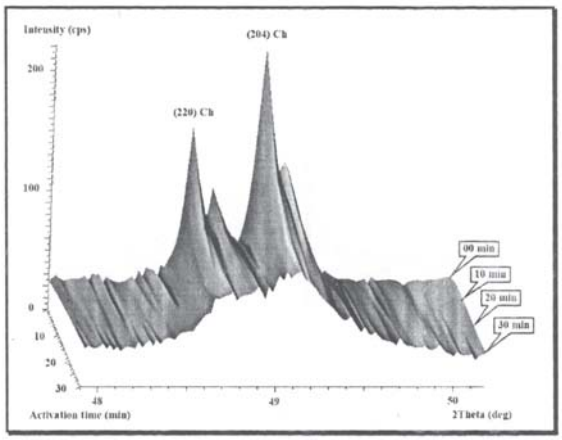

Fig. 12. 3D presentation of (220) and (204) chalcopyrite diffraction peaks for as received and milled samples vs. activation time

Regarding the lattice parameters of chalcopyrite, their value remains almost constant after 30 min of milling. It is found that crystallite size decreases exponentially with increasing time of mechanical activation but tends to a limit value when the activation time increases greatly. In our experiment this limit value seems to be about 20 nm.

The chosen function to describe average crystallite size is in the form:

$$D(t) = D_\infty + (D_0 - D_\infty)\exp(-kt) = D_\infty + (D_0 - D_\infty)\exp(-t/T) \quad (4)$$

where:

D(t) means isotropic average crystallite size in nm after t min of activation;

D_∞ is the limit value of crystallite size when $t \to \infty$;

D_0 is the initial value of crystallite size when $t = 0$;

t is the milling duration expressed in min;

$T = 1/k$; has the meaning of time constants (expressed in min) that characterize the activation process, depending on the milling parameters and also on the properties of milled mineral.

In our study the following expression for chalcopyrite isotropic crystallite size vs. activation time was found:

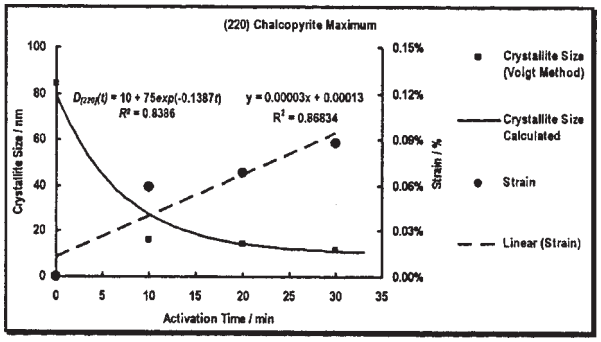

a

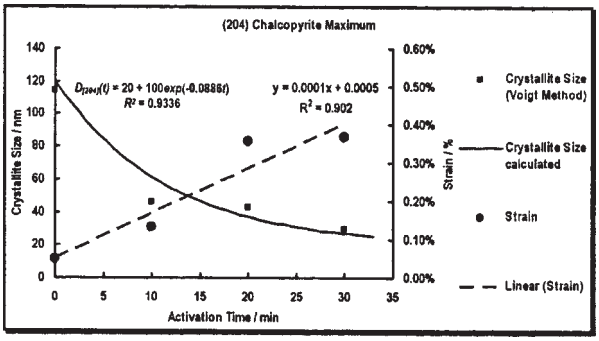

b

Fig. 13. Average crystallite size and lattice strain in [220] (a) and [204] (b) chalcopyrite directions vs. activation time

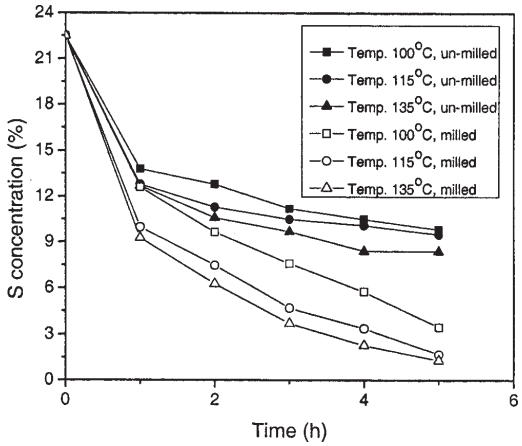

Fig. 14. Sulphur concentration for copper concentrate before and after mechanochimical treatment for 100, 115 and 135°C

$$D_{iso}(t) = 20 + 70\exp(-0.0837t) \quad (5)$$

with a good value for coefficient of determination (R - squared value): $R^2 = 0.9287$.

The time constant of activation process was found approximately: $T \approx 12$ min

With WinFit software, the experimental peaks are fit analytically using asymmetric Pearson VII functions. They can be corrected for instrumental broadening and decomposed into two components: Gaussian and

Lorentzian. Gaussian contribution characterises the effect on crystallites size and Lorentzian contribution characterises the effect of microstrain on the breadth of diffraction peaks. Thus, determining Pearson VII functions specific to each diffraction maximum allows calculation of the average size of crystallites and microstrain on the different crystallographic directions.

For this purpose the (220) and (204) diffraction peaks of chalcopyrite were selected because they are not altered by overlapping with the peaks of other minerals (fig. 12). Figure 12 provides a 3D representation of (220) and (204) diffraction peaks for chalcopyrite versus activation time, well highlighting trends between scans. It may be noted that the increase of milling time leads to loss in peaks' height simultaneously with increasing their breadth. This confirms the effects induced by mechanical activation: a decrease in average crystallite size and lattice strain occurrence.

The results of this approach are given in figure 13 a and b. It once again confirms the exponential decrease of crystallite size with increasing mechanical activation time. At the same time, lattice strain increases approximately linear.

Influence of mechanical activation on oxidation of metal sulphides from the copper concentrate

Chalcopyrite is oxidising in weak alkaline media in presence of oxygen from the air with CuO formation:

$$2CuFeS_2 + 4Na_2CO_3 + 8.5O_2(g) \rightleftarrows 2CuCO_3 + Fe_2O_3 + 4Na_2SO_4 + 2CO_2(g) \quad (6)$$

$$CuCO_3 \rightleftarrows CuO + CO_2(g) \quad (7)$$

In the same time secondary reactions may occur:

$$2CuFeS_2 + 8.5O_{2(g)} + 2H_2O \rightleftarrows 2CuSO_4 + Fe_2O_3 + 2H_2SO_4 \quad (8)$$

$$CuSO_4 + Na_2CO_3 \rightleftarrows CuCO_3 + Na_2SO_4 \quad (9)$$

$$6CuFeS_2 + Fe_2O_3 + 25.5O_{2(g)} \rightleftarrows 6CuO + 4Fe_2(SO_4)_3 \quad (10)$$

$$ZnS + Na_2CO_3 + 2O_2(g) \rightleftarrows ZnCO_3 + Na_2SO_4 \quad (11)$$

$$ZnCO_3 \rightleftarrows ZnO + CO_2(g) \quad (12)$$

In the presence of ferric oxide Fe_2O_3, the formed zinc oxide can react towards the formation of franklinite, according to the reaction below, which is undesired because this compound is very stable:

$$ZnO + Fe_2O_3 \rightleftarrows ZnFe_2O_4 \quad (13)$$

The lead is found in the concentrate as galena, PbS. In alkaline media PbS is oxidised to carbonate or basic lead and sodium carbonate.

$$PbS + Na_2CO_3 + 2O_2(g) \rightleftarrows PbCO_3 + Na_2SO_4 \quad (14)$$

$$4PbS + 5Na_2CO_3 + 8O_2(g) + H_2O \rightleftarrows 2NaOH^* 2PbCO_3 + 4Na_2SO_4 + CO_2(g) \quad (15)$$

Iron sulphide is oxidised in air presence with formation of hematite.

$$2FeS_2 + 4Na_2CO_3 + 7.5O_2(g) \rightleftarrows Fe_2O_3 + 4Na_2SO_4 + 4CO_2(g) \quad (16)$$

$$2FeS_2 + 7.5O_{2(g)} + 4H_2O \rightleftarrows Fe_2O_3 + 4H_2SO_4 \quad (17)$$

The resulted sulphuric acid is neutralized by the excess sodium carbonate as it follows:

$$H_2SO_4 + Na_2CO_3 \rightleftarrows Na_2SO_4 + H_2O + CO_2(g) \quad (18)$$

In the same time it is possible to obtain basic iron oxides as goethite.

$$2Fe_2(SO_4)_3 + 8H_2O \rightleftarrows 4FeOOH + 6H_2SO_4 \quad (19)$$

The sulphur concentration of the un-milled and milled concentrate for different temperatures is presented in figure 14.

It can be observed that an increase on the specific surface of copper concentrate from 0.1 to 4.33 m^2/g leads to a 3-fold decrease of the sulphur concentration at 100°C and approximately 6.5-fold at 135°C. In the same time, it is observed that the milling is also beneficial by shortening the reaction times: for a leaching temperature of 100°C, the un-milled sample required 5h whereas the milled sample only 2h, to attain the same values of sulphur concentration.

Conclusions

Mechanochemical activation of copper concentrate in an attrition mill for 30 min resulted to a decrease of the mean particle size d50 from 99 μm to 12 μm.

The calculated specific surface is increasing from 0.11 m^2/g before milling to 4.33 m^2/g after 30 min of activation.

The specific milling energy is increasing from 76, to 152 and 229 $KWh*t^{-1}$, for 10, 20 and 30 min respectively. The milling process becomes more energy demanding as the particle size distribution is decreasing.

Based on XRD structural analysis, it was found that chalcopyrite is the major mineral in copper concentrate and that copper is almost entirely bound in chalcopyrite.

Regarding the micro-structural changes occurring during the mechanical activation of chalcopyrite, it was found that the average crystallite size decreases versus mechanical activation time following an exponential trend towards a limit value. The limit value of crystallite size and the time constant characterizing the ball milling process depends on both the setup parameters of attrition mill and the milled mineral properties. Assuming spherical or equiaxed crystallites, the limit value of crystallite size is about 20 nm, and the time constant is 12 min. The lattice parameters of tetragonal chalcopyrite unit cell remains almost constant after 30 min of milling. The enhanced structural disorder of chalcopyrite is also highlighted by the linear increase of lattice strain with the milling time.

By increasing the surface area and the structural disorder in crystals, the mechanochemical treatment of copper concentrate is improving the leaching of metal sulphides, by lowering the reaction temperature and increasing the reaction rates.

References

1.MOSKALYK, R.R.ALFANTAZI, A.M., Review of copper pyrometallurgical practice: today and tomorrow. Miner. Eng., **16**(10), 2003, p. 893-919.

2.SASIKUMAR, C., SRIKANTH, S., MUKHOPADHYAY, N.K.MEHROTRA, S.P., Energetics of mechanical activation - Application to ilmenite. Miner. Eng., **22**(6), 2009, p. 572-574.

3.STEINIKE, U.TKÁČOVÁ, K., Mechanochemistry of Solids—Real Structure and Reactivity. J Mater. Synth. Proces., **8**(3), 2000, p. 197-203.

4.SASIKUMAR, C., RAO, D.S., SRIKANTH, S., RAVIKUMAR, B., MUKHOPADHYAY, N.K.MEHROTRA, S.P., Effect of mechanical activation on the kinetics of sulfuric acid leaching of beach sand ilmenite from Orissa, India. Hydrometallurgy, **75**(1-4), 2004, p. 189-204.

5.ACHIMOVICOVÁ, M.BALÁZ, P., Influence of mechanical activation on selectivity of acid leaching of arsenopyrite. Hydrometallurgy, **77**(1-2), 2005, p. 3-7.
6.WELHAM, N.J., The effect of extended milling on minerals. Vol. 90. 1997, Montreal, PQ, CANADA: Canadian Institute of Mining, Metallurgy and Petroleum.
7.WELHAM, N.J., Enhanced dissolution of tantalite/columbite following milling. Int. J Miner. Process., **61**(3), 2001, p. 145-154.
8.BALÁZ, P., Chapter 1 Mechanochemistry and mechanical activation of solids, in Process Metallurgy. 2000, Elsevier. p. 1-14.
9.HU, H.-P., CHEN, Q.-Y., YIN, Z.-L., HE, Y.-H.HUANG, B.-Y., Mechanism of mechanical activation for sulfide ores. Transactions of Nonferrous Metals Society of China, **17**(1), 2007, p. 205-213.
10.TKÁCOVÁ, K.BALÁZ, P., Reactivity of mechanically activated chalcopyrite. Int. J Miner. Process., **44-45**1996, p. 197-208.
11.ACHIMOVIČOVÁ, M., BALÁ•, P.BRIANČIN, J., The influence of mechanical activation of chalcopyrite on the selective leaching of copper by sulphuric acid, in Metalurgija. 2006. p. 9-12.
12.CONSTANTIN, I., TALOI, D.VLADUTIU, L., Procese de difuzie si transfer de masa, ed. E.D.s. Pedagogica. 2005, Bucuresti.
13.GODOČIKOVÁ, E., LEŠKO, M.BALÁ•, P., Usage of a statistical method of designing factorial experiments in the mechanical activation of a complex CuPbZn sulphide concentrate. Acta Montan. Slovaca, **8**(2-3), 2003, p. 134-138.
14.*** INTERNATIONAL CENTRE FOR DIFFRACTION DATA, ICDD Database, Powder diffraction file. 2006.
15.KRUMM, S., WinFit 1.0 - A computer Program for X-ray Diffraction Line Profile Analysis. 1994: Erlagen, Germany.
16.*** NATIONAL INSTITUTE OF STANDARDS AND TECHNOLOGY, Certificate of Analysis: Standard Reference Material 1976 - Instrument Sensitivity Standard for X-Ray Powder Diffraction. 2007, Gaithersburg, USA.

Manuscript received: 26.09.2011